

Crystallization, X-ray characterization and selenomethionine phasing of Mlc1p bound to IQ motifs from myosin V

Mohammed Terrak, Ludovic R. Otterbein, Guanming Wu, Lakshmi A. Palecanda, Renne C. Lu and Roberto Dominguez*

Boston Biomedical Research Institute, 64 Grove Street, Watertown, Massachusetts 02472, USA

Correspondence e-mail: dominguez@bbri.org

Mlc1p is a calmodulin-like protein from the budding yeast *Saccharomyces cerevisiae*, where it has been identified as a subunit of a class V myosin, Myo2p, and a binding partner of an IQGAP-like protein, Iqg1p. Through its interactions with these two proteins, Mlc1p plays a role in polarized growth and cytokinesis. Mlc1p has been crystallized in complexes with four different IQ target motifs from the neck region of Myo2p: IQ2, IQ3, IQ4 and IQ2–IQ3 (referred to as IQ2,3). Electron-density maps for two of the complexes (Mlc1p–IQ4 and Mlc1p–IQ2,3) were obtained from multiple anomalous dispersion (MAD) experiments based on selenomethionine derivatives. The other two structures (Mlc1p–IQ2 and Mlc1p–IQ3) were determined by molecular replacement using the partially refined structure of Mlc1p–IQ2,3 as a search model.

Received 6 May 2002
Accepted 5 August 2002

1. Introduction

Mlc1p is a calmodulin-like protein that was first identified as a light chain for the *Saccharomyces cerevisiae* class V myosin Myo2p (Stevens & Davis, 1998). Myo2p is essential for growth of *S. cerevisiae*, where it localizes to the bud tip during bud formation and to the bud neck during cytokinesis (Brockerhoff *et al.*, 1994; Lillie & Brown, 1994). Myosins of different classes bind a varying number of light chains that can be either calmodulin or calmodulin-related proteins such as Mlc1p (Sellers, 2000). Binding of the light chains to the heavy chains of myosins takes place through specific target sequences known as IQ motifs. These motifs are ~25 amino-acid regions that conform to the consensus sequence (I,L,V)QxxxR-xxx(R,K) (reviewed by Bahler & Rhoads, 2002). The light-chain-binding domain (or neck region) of Myo2p, in particular, holds six such IQ motifs. In addition to myosins, IQ motifs are also present in a number of neuronal growth proteins, voltage-operated channels and certain signalling molecules (Bahler & Rhoads, 2002).

The finding that disruption of the *MLC1* gene in *S. cerevisiae* causes a cytokinesis defect (Stevens & Davis, 1998) which is independent of its Myo2p-binding activity led to the search for different binding partners of Mlc1p (Shannon & Li, 2000). Thus, it was found that Mlc1p also binds to a class II myosin (Myo1p) in late mitosis and an IQGAP-like protein (Iqg1p) during cytokinesis (Boyne *et al.*, 2000; Shannon & Li, 2000). Binding of Mlc1p to Iqg1p is also mediated by interactions with IQ

motifs, of which this protein contains at least nine copies. This interaction appears to help recruit Iqg1p to the bud neck (Shannon & Li, 2000; Boyne *et al.*, 2000).

Together, these results are consistent with a key role for Mlc1p in cytokinesis. The functional activity of Mlc1p is dependent upon its ability to interact with different effector proteins that contain multiple copies of related, albeit different, IQ target sequences. To understand the nature of these interactions and how they may mediate the function of Mlc1p, we are studying the crystal structures of complexes of Mlc1p with various IQ motifs. Here, we report the crystallization and structure determination of complexes of Mlc1p with IQ2, IQ3, IQ4 and IQ2–IQ3 in tandem (hereafter referred to as IQ2,3) of the heavy chain of Myo2p.

2. Material and methods

2.1. Preparation of Mlc1p and IQ motifs

Wild-type Mlc1p (Swiss-Prot entry P53141; 16 444 Da; 149 amino acids) was cloned into vector pAED4 and expressed in *Escherichia coli* (grown in Luria–Bertani medium) using the T7 promoter system (Studier & Moffatt, 1986). Mlc1p contains a single methionine residue, Met109. A mutant of Mlc1p, Ile64→Met (henceforth referred to as I64M), was generated to facilitate the resolution of the structure. I64M Mlc1p was produced using the Quik-change site-directed mutagenesis kit (Stratagene, La Jolla, CA, USA). A selenomethionine (SeMet) derivative of I64M Mlc1p was expressed in SeMet-supplemented

minimal medium using the same expression system as for the wild-type protein (Doublet, 1997). The presence of the SeMet substitution was confirmed by mass spectrometry. The protein solutions were loaded onto a Whatman DE52 column and eluted with a 20–100 mM stepwise gradient of sodium chloride. Both Mlc1p and the I64M mutant emerge from the column at about 50 mM salt concentration. Synthetic peptides, corresponding to IQ2, IQ3, IQ4 and IQ2,3 of Myo2p (Fig. 1) were produced on an ABI 431 peptide synthesizer using Fmoc chemistry. The peptides were then cleaved from the resins and purified by HPLC. The identity and purity of the peptides were confirmed by mass spectrometry.

Prior to crystallization, Mlc1p and I64M Mlc1p (SeMet derivative) were dialyzed against 20 mM Tris-HCl pH 8.0, 1 mM EDTA and 100 mM sodium chloride and mixed at a concentration of ~ 0.5 mg ml⁻¹ with the IQ peptides in a 1:1.5 molar ratio. The Mlc1p-IQ complexes were then dialyzed against 5 mM sodium acetate pH 4.0, 1 mM calcium chloride, 1 mM DTT buffer and concentrated to ~ 10 mg ml⁻¹ using Centricon microconcentration devices (Amicon Inc., Beverly, MA, USA).

3. Results and discussion

3.1. Crystallization

The crystallization conditions for Mlc1p-IQ2 and Mlc1p-IQ4 were derived from condition number 6 of the PEG/Ion and condition number 14 of the Crystal Screen 2

formulations from Hampton Research (Laguna Niguel, CA, USA), respectively. Although the crystals of Mlc1p-IQ2 diffracted well (see below), they were difficult to reproduce. In subsequent crystallization experiments, we could only obtain crystals of Mlc1p-IQ2 of small size and poor quality. The crystallization conditions for Mlc1p-IQ3 and Mlc1p-IQ2,3 were obtained from a polyethylene glycol 5000 monomethyl ether screening formulation developed in our laboratory. All the crystals were obtained at a temperature of 293 K. Pictures of the crystals are shown in Fig. 1. Table 1 summarizes the best crystallization conditions for each of the Mlc1p-IQ complexes.

Prior to X-ray data collection, the crystals were transferred for a split second into cryoprotectant solutions containing, in addition to the crystallization buffer, 12–20% glycerol. The crystals were then flash-frozen in propane-filled vials, which were finally stored in a large liquid-nitrogen dewar. Freezing improved the data quality and resolution of all the crystals except those of Mlc1p-IQ4 (see below).

3.2. Data collection and MAD phasing

High-resolution data sets were collected at 100 K for complexes of Mlc1p with IQ2 and IQ2,3 using the BioCARS beamlines 14-BM-D and 14-BM-C (APS, Argonne). Table 2 summarizes the data-collection statistics. Crystals of Mlc1p-IQ3, however, do not diffract X-rays well. The best data set for this complex, collected to 3.0 Å resolution, was obtained from an extensive

Table 1

Crystallization of complexes of Mlc1p with myosin V heavy chain IQ fragments.

Mlc1p-IQ2	20% (w/v) polyethylene glycol 3350, 0.2 M sodium chloride
Mlc1p-IQ3	25% polyethylene glycol 5000 monomethyl ether, 20 mM sodium acetate pH 3.8
Mlc1p-IQ4 and I64M Mlc1p-IQ4 (SeMet derivative)	2.2 M ammonium sulfate, 0.2 M potassium sodium tartrate tetrahydrate, 0.1 M trisodium citrate dihydrate pH 5.6
Mlc1p-IQ2,3 and I64M Mlc1p-IQ2,3 (SeMet derivative)	23% polyethylene glycol 5000 monomethyl ether, 0.3 M potassium fluoride

screening of crystals using our home source (Rigaku RU-H3RH B X-ray generator, MAR345 imaging-plate detector, Oxford Cryostream low-temperature system, and Charles Supper double-mirror X-ray focusing system). All data sets were indexed and scaled with the programs *DENZO* and *SCALEPACK* (Otwinowski & Minor, 1997).

Crystals of Mlc1p-IQ4, on the other hand, diffract significantly better (2.1 Å resolution and low mosaicity) at room temperature and using our home source. Indeed, a broad search for cryoprotectant conditions, which included growing the crystal in the presence of various cryoprotectants, failed to produce suitable cryofreezing conditions. The major problems encountered were a dramatic increase in mosaicity and a lower diffraction resolution. However, in order to solve the structure of Mlc1p-IQ4 we performed an SeMet MAD experiment, which required freezing in order to limit radiation damage to the I64M Mlc1p-IQ4 crystals. In this case, the crystals were flash-cooled using glycerol as a cryoprotectant. The three-wavelength MAD experiment data (Table 3) were collected at BioCARS beamline 14-BM-D (APS, Argonne). We found that in addition to a higher mosaicity and lower resolution, the frozen crystals experienced a space-group and unit-cell change (see Tables 2 and 3). Note that when collected at room temperature, the SeMet I64M mutant had the same unit cell as the wild-type protein, indicating that the change in the unit cell arose from a freezing artifact. There are two Mlc1p-IQ4 complexes in the asymmetric unit of the frozen crystals (compared with a single complex in the crystals collected at room temperature). Nevertheless, we were able to find the positions of the four Se atoms in the asymmetric unit (two per Mlc1p-IQ4 complex) with the program *SnB* (Weeks & Miller, 1999). The positions and occupancies of the Se atoms were refined with the program *MLPHARE* (Collabora-

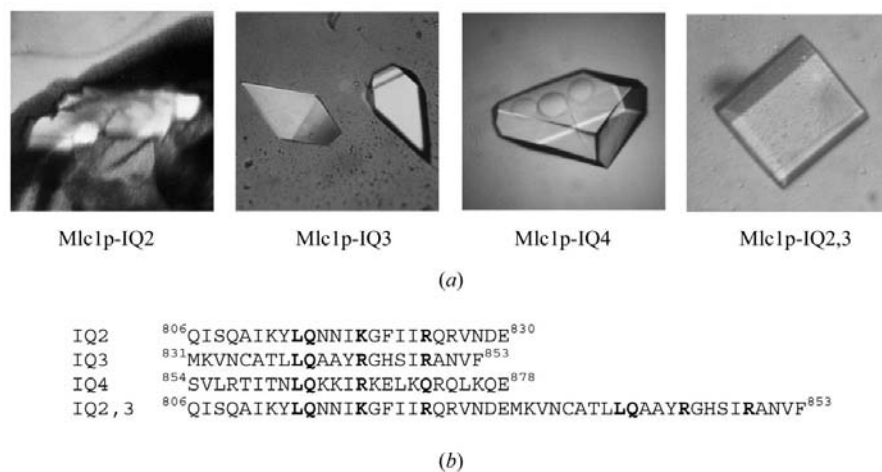


Figure 1

(a) Crystals of complexes of Mlc1p with IQ target motifs from the myosin V heavy chain. Each IQ motif binds one molecule of Mlc1p. There are therefore two molecules of Mlc1p bound to the longer IQ2,3 fragment. The sequences of the IQ motifs of Myo2p that were co-crystallized with Mlc1p are shown in (b). The amino acids shown in bold represent generally conserved positions. Notice that crystals of Mlc1p-IQ2 grow from protein precipitates and are difficult to reproduce. The crystal of Mlc1p-IQ2 shown in (a) was 'operated' using a cat whisker. Three single crystals were obtained in this way. The 1.65 Å resolution data set of Mlc1p-IQ2 described in Table 2 was collected from one of these crystals. The crystal of Mlc1p-IQ4 shown here has been featured on the cover of the Hampton Research Catalogue.

tive Computational Project, Number 4, 1994), which resulted in a first set of phases to 3.0 Å resolution. The *MLPHARE* phases were further refined and extended to 2.6 Å resolution (Fig. 2) with the program *DM* (Cowtan & Main, 1998). Note that this 2.6 Å resolution data set from the SeMet frozen crystals was obtained by merging, with the

program *SCALEPACK* (Otwinowski & Minor, 1997), all the anomalous diffraction data collected for three different wavelengths (Table 3) as a single non-anomalous

data set (Table 2). The N- and C-terminal domains of Mlc1p are oriented slightly differently in the two complexes of the asymmetric unit in the frozen crystals, which

Table 2
Data-collection statistics.

Values in parentheses are for the last resolution shell.

	Mlc1p-IQ2	Mlc1p-IQ3	Mlc1p-IQ4	Mlc1p-IQ4 (I64M, SeMet)	Mlc1p-IQ2,3
X-ray source	14-BM-D BioCARS, APS	Home source	Home source	14-BM-D BioCARS, APS	14-BM-C BioCARS, APS
Space group	$P2_12_12_1$	$P4_12_12$	$P2_12_12$	$P2_12_12_1$	$P2_12_12$
Unit-cell parameters (Å, °)					
<i>a</i>	43.6	54.7	48.5	46.79	80.0
<i>b</i>	56.5	54.7	121.5	56.36	64.2
<i>c</i>	56.9	120.9	29.1	115.9	72.8
$\alpha = \beta = \gamma$ (°)	90.0	90.0	90.0	90.0	90.0
V_M^\dagger (Å ³ Da ⁻¹)	1.82	2.39	2.22	2.0	2.46
Solvent content (%)	32.4	48.6	44.5	37.7	50.0
Resolution range (Å)	25.0–1.65 (1.71–1.65)	38.0–3.0 (3.11–3.0)	45.0–2.1 (2.18–2.1)	50.0–2.6 (2.71–2.6)	40.0–2.0 (2.01–2.0)
Completeness (%)	97.1 (86.0)	95.7 (72.2)	99.7 (98.5)	93.1 (74.2)	99.5 (99.1)
Total No. of observations	176831	129625	109834	371709	1650909
No. of unique observations	17258	3865	10540	9242	25861
Redundancy	10.3	33.5	10.4	40.2	63.8
$R_{\text{merge}}^\ddagger$ (%)	3.6 (20.0)	14.0 (40.2)	7.5 (36.0)	8.9 (28.0)	9.8 (42.3)
R_{merge}^\S (%)	3.2 (23.1)	8.5 (37.2)	6.3 (32.7)	9.1 (29.2)	8.7 (37.2)
Average $I/\sigma(I)$	25.6 (6.1)	9.6 (3.8)	15.0 (4.2)	37.1 (7.5)	17.0 (5.0)
Crystal mosaicity (°)	0.7	0.2	0.24	1.21	0.9

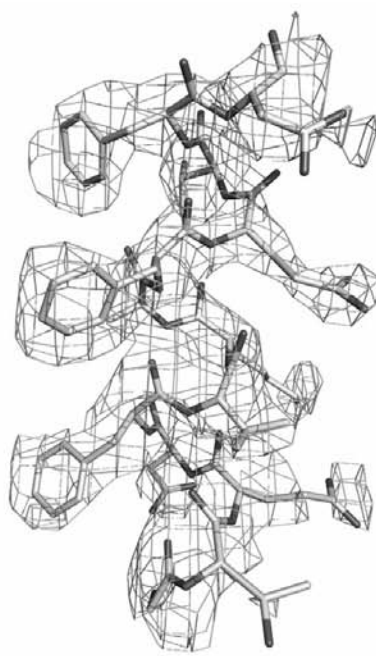
$\dagger V_M$, Matthews coefficient = unit-cell volume/No. of macromolecules in the unit cell. $\ddagger R_{\text{merge}} = \sum |I - \langle I \rangle| / \sum I$, where I is the intensity of an individual reflection and $\langle I \rangle$ is its mean value. $\S R_{\text{merge}}^\S = \sum (I - \langle I \rangle)^2 / \sum I^2$.

Table 3
Multiple anomalous dispersion (MAD) phasing statistics.

Values in parentheses are for the last resolution shell.

	Mlc1p I64M-IQ2,3 (SeMet derivative)			Mlc1p I64M-IQ4 (SeMet derivative)		
X-ray source	F2, CHESS			14-BM-D, BioCARS, APS		
Space group	$P2_12_12_1$			$P2_12_12_1$		
Unit-cell parameters						
<i>a, b, c</i> (Å)	79.38, 63.95, 72.89			46.79, 56.36, 115.9		
α, β, γ (°)	90.0, 90.0, 90.0			90.0, 90.0, 90.0		
Data-collection statistics						
Wavelength (Å)	$\lambda_1 = 0.97937$	$\lambda_2 = 0.9792$	$\lambda_3 = 0.932209$	$\lambda_1 = 0.97811$	$\lambda_2 = 0.97788$	$\lambda_3 = 0.94071$
Resolution range (Å)	60.0–2.5 (2.59–2.5)	60.0–2.5 (2.59–2.5)	60.0–2.5 (2.59–2.5)	50.0–2.9 (3.0–2.9)	50.0–2.9 (3.0–2.9)	50.0–2.9 (3.0–2.9)
Completeness (%)	99.9 (98.6)	99.9 (99.2)	100.0 (99.9)	88.8 (78.2)	92.6 (87.3)	89.9 (79.2)
Total No. of observations	169059	173600	182011	76136	106220	76062
No. of unique observations	13352	13367	13599	6339	6579	6448
Redundancy	12.7	13.0	13.4	12.0	16.2	11.8
R_{merge}^\dagger (%)	6.8 (36.3)	8.1 (35.4)	7.1 (38.2)	6.9 (16.7)	9.5 (21.3)	7.2 (20.2)
$R_{\text{merge}}^\ddagger$ (%)	5.8 (29.4)	7.1 (29.1)	5.2 (34.1)	6.6 (18.7)	13.0 (22.5)	7.2 (20.1)
Average $I/\sigma(I)$	17.3 (8.0)	15.1 (7.9)	17.6 (8.1)	21.6 (6.9)	19.2 (5.9)	21.0 (6.8)
Crystal mosaicity (°)	1.15			1.21		
Phasing statistics						
Phasing resolution (Å)	20.0–3.0	20.0–3.0	20.0–3.0	20.0–3.0	20.0–3.0	20.0–3.0
No. of heavy atoms	–	4	4	4	4	–
Phasing power §						
Acentric	–	0.3	0.74	1.05	0.96	–
Centric	–	0.2	0.52	1.02	0.79	–
R_{cullis}^\P						
Acentric	–	0.99	0.93	0.76	0.80	–
Centric	–	0.97	0.84	0.68	0.742	–
Anomalous	–	0.89	0.88	0.77	0.82	–
Figure of merit	0.37			0.35		
Phase extension and refinement ††						
Resolution (Å)	50.0–2.0			50.0–2.4		
Figure of merit	0.57			0.38		

$\dagger R_{\text{merge}} = \sum |I - \langle I \rangle| / \sum I$, where I is the intensity of an individual reflection and $\langle I \rangle$ is its mean value. $\ddagger R_{\text{merge}}^\ddagger = \sum (I - \langle I \rangle)^2 / \sum I^2$. \S Phasing power = $(F_H/\text{lack of closure})$, where F_H is the calculated heavy-atom structure-factor amplitude. $\P R_{\text{cullis}} = (\text{lack of closure})/(\text{isomorphous difference})$. †† Phase extension and refinement were performed with the program *DM* (Cowtan & Main, 1998), using options SOLV, HIST and MULT.



(a)



(b)

Figure 2
Representative sections of the *DM*-refined SeMet MAD maps of the Mlc1p-IQ4 (a) and Mlc1p-IQ2,3 (b) complexes calculated at 2.9 Å resolution and displayed at 1.2 σ . The maps are superimposed on the partially refined atomic models of the structures.

explains why non-crystallographic symmetry averaging was not applied during phase refinement. Nonetheless, the *DM* electron-density map was of excellent quality and was used to construct an incomplete model of the Mlc1p–IQ4 complex (Fig. 2), which was subsequently used to find a molecular-replacement solution in the unit cell of the crystals collected at room temperature, which diffracted to 2.1 Å resolution. We are currently working on the refinement of this structure.

It became clear immediately that the structure of Mlc1p–IQ4 presented some major differences with respect to those of the other three Mlc1p–IQ complexes and that molecular replacement could not be used toward solving these structures. Using the same SeMet derivative of the I64M mutant of Mlc1p, we were able to grow crystals of the complex with IQ2,3. A three-wavelength MAD experiment (Table 3) was conducted at beamline F2, CHESS (Ithaca, NY). The data sets were indexed and scaled with the programs *DENZO* and *SCALEPACK* (Otwinowski & Minor, 1997). The four Se atoms in the asymmetric unit of the crystals (containing two molecules of Mlc1p bound to IQs 2 and 3) were found with the program *SAPI* (Quan Hao, MacCHESS, Cornell University) and refined with the program *MLPHARE* (Collaborative Computational Project, Number 4, 1994) to

3.0 Å resolution. The phases were further refined and extended to 2.0 Å resolution with the program *DM* (Cowtan & Main, 1998). Fig. 2 shows a representative section of the experimental electron-density map. The structure is currently being refined. Molecular-replacement solutions of the structures of Mlc1p–IQ2 and Mlc1p–IQ3 have been also found using the partially refined structure of the Mlc1p–IQ2,3 complex as a search model.

In summary, we have described here the crystallization, high-resolution data collection and phasing of four complexes of Mlc1p bound to IQ motifs 2, 3, 4 and 2–3 in tandem from the neck region of Myo2p, a class V myosin. The structures, which are currently being refined, are beginning to reveal unexpected features of the interaction of Mlc1p with IQ target motifs. For instance, as a result of slight variations in the sequence of the bound IQ motifs, the conformation of Mlc1p varies dramatically. These target-dependent conformational differences are likely to play an important part in the ability of Mlc1p to recruit Iqg1p during cytokinesis.

Supported by NIH grant R01 AR46524 to RD. Use of the Advanced Photon Source was supported by the US Department of Energy, Basic Energy Sciences, Office of Science under contract No. W-31-109-Eng-

38. Use of the BioCARS facilities was supported by NIH grant RR07707. Use of the CHESS and MacCHESS facilities was supported by the NSF (award DMR 97-13424) and NIH (award RR-01646), respectively. We would like to thank the staff members at BioCARS and MacCHESS for assistance during data collection.

References

- Bahler, M. & Rhoads, A. (2002). *FEBS Lett.* **513**, 107–113.
- Boyne, J. R., Yusuf, H. M., Bieganowski, P., Brenner, C. & Price, C. (2000). *J. Cell Sci.* **113**, 4533–4543.
- Brockerhoff, S. E., Stevens, R. C. & Davis, T. N. (1994). *J. Cell Biol.* **124**, 315–323.
- Collaborative Computational Project, Number 4 (1994). *Acta Cryst.* **D50**, 760–763.
- Cowtan, K. & Main, P. (1998). *Acta Cryst.* **D54**, 487–493.
- Doublet, S. (1997). *Methods Enzymol.* **276**, 494–523.
- Lillie, S. H. & Brown, S. S. (1994). *J. Cell Biol.* **125**, 825–842.
- Otwinowski, Z. & Minor, W. (1997). *Methods Enzymol.* **276**, 307–326.
- Sellers, J. R. (2000). *Biochim. Biophys. Acta*, **1496**, 3–22.
- Shannon, K. B. & Li, R. (2000). *Curr. Biol.* **10**, 727–730.
- Stevens, R. C. & Davis, T. N. (1998). *J. Cell Biol.* **142**, 711–722.
- Studier, F. W. & Moffatt, B. A. (1986). *J. Mol. Biol.* **189**, 113–130.
- Weeks, C. M. & Miller, R. (1999). *J. Appl. Cryst.* **32**, 120–124.